Calculation of positron states in C_{60}

Shoji Ishibashi[1] and Masanori Kohyama[1,2]
[1]*Research Institute for Computational Sciences (RICS), National Institute of Advanced Industrial Science and Technology (AIST), Central 2, 1-1-1 Umezono, Tsukuba, Ibaraki 305-8568, Japan*
[2]*Special Division of Green Life Technology, National Institute of Advanced Industrial Science and Technology (AIST). 1-8-31 Midorigaoka, Ikeda, Osaka 563-8577, Japan*
(Received 13 November 2002; revised 17 January 2003; published 18 March 2003)

Positron energy levels and distributions in the C_{60} crystal have been calculated based on the self-consistent electronic structure obtained with an *ab initio* plane-wave pseudopotential calculation. For the correlation energy between electrons and a positron, we used both the local-density approximation (LDA) and generalized gradient approximation (GGA). Although the results obtained with these two approximations are similar to each other, there are some quantitative differences. In the LDA positron band structure, the width of the lowest band is narrower and the energy gap between the lowest and second lowest bands is larger than those for the GGA result. We have examined lattice expansion effects also. The present result is expected to throw light on the positron behavior in the C_{60} crystal.

DOI: 10.1103/PhysRevB.67.113403 PACS number(s): 71.60.+z, 78.70.Bj

In the solid form, the C_{60} molecules are arranged at lattice points of the face-centered-cubic (fcc) structure.[1] There are three kinds of open spaces in the crystal, the octahedral and tetrahedral interstices, which always exist in the fcc structure, and the inner space of the C_{60} molecule.

The positron has a positive charge and tends to escape from nuclei. As a result, positrons are distributed in open spaces in condensed matter. At which site are positrons distributed in the C_{60} crystal? Many studies have been performed in recent years. From the theoretical side, the positron distribution has been calculated with the superposed-neutral-atom model,[2–4] or with the positron potential constructed from more precise electron-charge-density data.[5,6] Most results predict that positrons are predominantly distributed at the octahedral site. One exception is the result obtained with the generalized gradient approximation (GGA) and the electron charge constructed as a superposition of the molecular orbitals.[6] In this result, the positron density maximum is located at the tetrahedral site. From the experimental side, the temperature variations of the positron lifetime were measured by several groups.[7–10] The positron lifetime increases with temperature increasing. The lattice dimension of the C_{60} crystal increases with temperature while the size of the C_{60} molecule itself is almost invariant. From these facts, it was concluded that positrons exist in the interstitial region. Sunder *et al.*[10] measured the positron lifetime up to 400 °C and interpreted its temperature variation by applying the two-state trapping model. They proposed that a thermally activated positron tunnels into the C_{60} cage with an activation energy of 0.45 eV.

In this work, we report the positron states (the ground state as well as a few excited states) calculated with the self-consistent electron density obtained by an *ab initio* calculation. Positron band structures and density distributions are shown. To describe the electron-positron correlation, we tested both the local-density approximation (LDA) and GGA expressions. We examined the lattice expansion effect on the positron states also.

The present calculation of the electronic structure of C_{60} is based on the norm-conserving pseudopotential method[11] within the LDA framework. We adopted the Ceperly-Alder correlation[12] parametrized by Perdew and Zunger.[13] As regards pseudopotentials, we used those proposed by Troullier and Martins[14] with the separable approximation[15] and the partial core correction.[16] To obtain the final converged wave function, the preconditioned conjugate gradient method[17] modified by Bylander *et al.*[18] with the charge mixing scheme by Kerker,[19] which has been shown to be suitable for large systems,[20] was used together with the Gaussian smearing technique.[21] The calculation was made on an assumed fcc structure that has the *Fm3* symmetry instead of the experimentally confirmed *Pa3* structure for computational simplicity. The direction of C_{60} molecules in the crystal does not affect the positron distribution much as shown in our previous paper.[22] C_{60} molecules with the C-C bond lengths of 1.45 Å and 1.39 Å are located at the fcc lattice points so that three of the twofold axes correspond to three crystallographic orthogonal axes. We used the room-temperature lattice constant $a=14.17$ Å or $1.02a$. The size of the C_{60} molecule was kept constant. The energy cutoff of plane waves was chosen to be 55 Ry. Two special k points were used when calculating the self-consistent charge density. With the obtained charge density, we calculated energy eigenvalues on additional k points in order to compare the present result with others. The present electronic band structure is in excellent agreement with that reported by Troullier and Martins.[23]

The potential for positrons was constructed from the obtained self-consistent charge density. The Hartree part was constructed from all electron data (frozen core and pseudovalence charge). The electron-positron correlation part was described within the LDA (Ref. 24) or GGA (Refs. 25 and 26) framework. For the latter case, we described the electron-positron correlation $E_{GGA}^{corr}(\mathbf{r})$ as

$$E_{GGA}^{corr}(\mathbf{r})=E_{LDA}^{corr}(\mathbf{r})\exp(-\alpha\epsilon)+c_2[1-\exp(-\alpha\epsilon)], \quad (1)$$

 ©2003 The American Physical Society

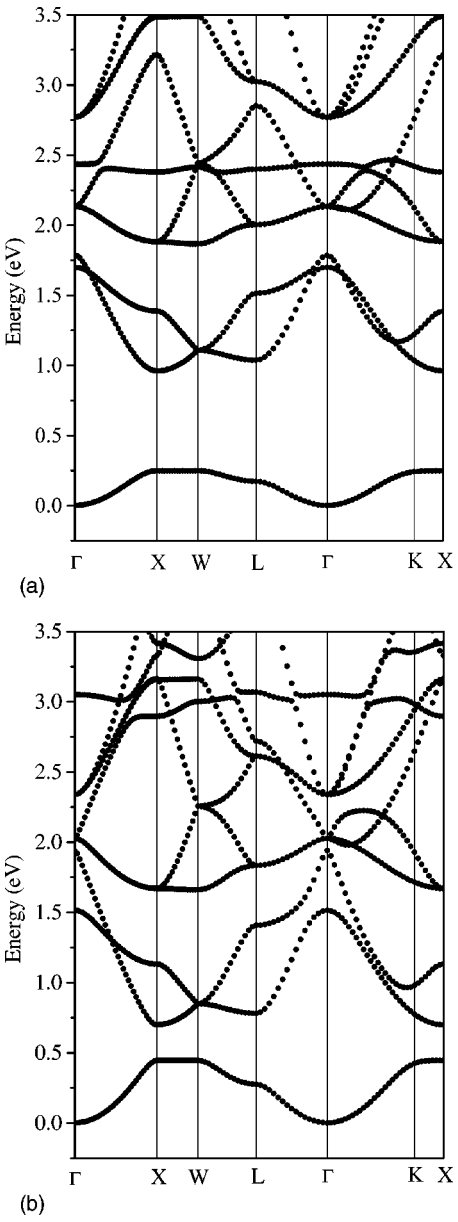

FIG. 1. Positron band structures obtained with (a) LDA and (b) GGA.

where definitions of symbols are the same as in Ref. 26 and $c_2=0.11$ Ry. Although the c_2 term is usually neglected, we have included this since its contribution seems significant for the present low-electron-density case. The positron wave functions were obtained with the same plane-wave basis and convergence method as was used in the electron-wave-function calculations.

Figure 1 represents the positron band structures for $a=14.17$ Å calculated with LDA [Fig. 1(a)] and GGA [Fig. 1(b)]. For both the cases, the maximum of the positron density distribution for the ground state (the lowest-band bottom at the Γ point) is located at the octahedral site as shown in Figs. 2(a) and 2(b), though there is a quantitative difference. The present GGA result is quite different from our previous one obtained with the superposed-molecular-orbital charge density.[6] Such a large difference with the GGA was reported

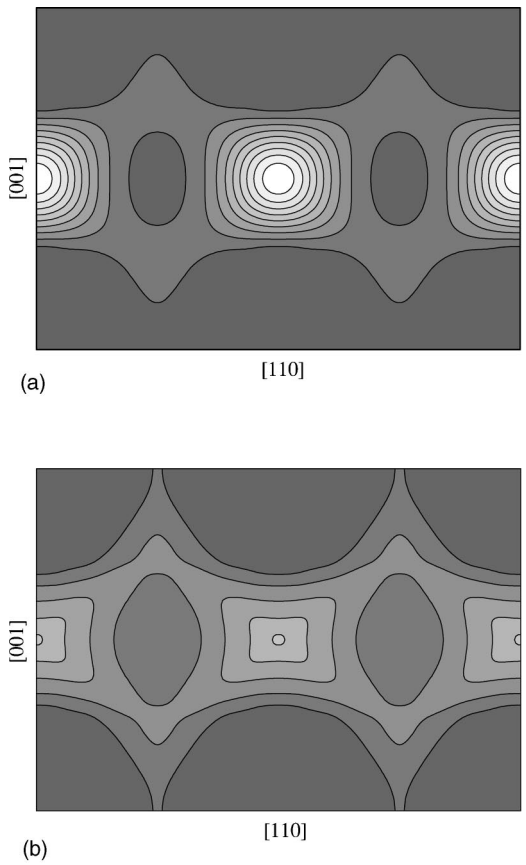

FIG. 2. Positron density distribution obtained with (a) LDA and (b) GGA. Bright parts represent higher values.

for carbon nanotube bundles also.[27] It would be due to the GGA sensitivity to details of the electronic structure, as mentioned in Refs. 25 and 26. As shown in Fig. 2, the relative amplitude at the tetrahedral site is higher for the GGA result than that for LDA. In other words, the positron ground state is less localized for the GGA result. This is reflected in the difference of the bandwidths. The bandwidths for the GGA is much wider than that for LDA. The positron density for the first excited state (the second band) at the Γ point has a maximum at the tetrahedral site. There is a direct band gap at the X point. The gap for the GGA is smaller than that for the LDA. The widths of the lowest-band and the band-gap values are listed in Table I. We calculated the positron distribution for some higher states. For example, the second excited state (the third band) at Γ is distributed at both the octahedral and the tetrahedral sites. The third to fifth excited states (the fourth to sixth bands) at Γ show p-like character located at

TABLE I. Positron band parameters in C_{60} for LDA, GGA ($\alpha=0.22$), and GGA2 ($\alpha=0.12$).

	LDA		GGA		GGA2	
	a	$1.02a$	a	$1.02a$	a	$1.02a$
$W_{\Gamma-W}$ (meV)	247	258	444	508	372	422
ΔE_X (meV)	713	632	255	101	399	257

TABLE II. Fraction f_{in} of positron density distribution inside the C_{60} cage for LDA. Values were evaluated at special points Γ, X, W, L, and K. n represents the band index and E_n is the corresponding energy eigenvalue in eV. Higher fraction values are underlined.

	Γ		X		W		L		K	
n	E_n	f_{in}	E_n	f_{in}	E_n	f_{in}	E_n	f_{in}	E_n	f_{in}
1	0.00	0.007	0.25	0.002	0.25	0.002	0.17	0.003	0.24	0.002
2	1.70	0.004	0.96	0.007	1.11	0.007	1.04	0.014	1.03	0.007
3	1.78	0.035	1.39	0.005	1.11	0.007	1.51	0.005	1.22	0.008
4	2.13	0.004	1.88	0.007	1.86	0.045	2.00	0.005	1.92	0.006
5	2.13	0.004	1.88	0.007	2.41	0.948	2.00	0.005	2.12	0.096
6	2.13	0.004	2.38	0.973	2.44	0.005	2.40	0.954	2.42	0.892
7	2.44	0.959	3.21	0.004	2.44	0.005	2.85	0.034	2.76	0.004
8	2.77	0.007	3.48	0.004	3.49	0.003	3.02	0.009	3.31	0.005
9	2.77	0.007	3.49	0.003	3.53	0.019	3.02	0.009	3.55	0.019
10	2.77	0.007	3.54	0.027	4.01	0.006	3.86	0.012	3.93	0.004

the octahedral site. In order to investigate states which have a maximum density inside the C_{60} molecule, we evaluated fractions of the positron density distribution inside the C_{60} cage (regarded as a sphere with a radius of 3.54 Å) at special points Γ, X, W, L, and K. The obtained values are listed in Tables II and III for LDA and GGA, respectively. Such a state is located at $\sim$2.4 eV for LDA or $\sim$3.0 eV for GGA above the ground state. These values are much higher than the activation energy of 0.45 eV proposed by Sundar *et al.*[10] The present calculation takes no structural relaxation due to positrons into account. There is a possibility that such a relaxation reduces the energy difference between the two states. Further work is needed.

The results for $1.02a$ are similar to those for $a=14.17$ Å, though there are several quantitative changes. As shown in Table I, for both the LDA and GGA cases, the bandwidth increases while the gap decreases with the lattice expansion. For the electron-band case, there is a general tendency that the bandwidth decreases with the lattice expansion because the overlap between atomic/molecular orbitals, which contributes to the band formation, decreases. In the present positron case, the situation is different. The octahedral site is the place at which positrons can stay farthest away from nuclei, and this site is favorable for positrons in terms of the electrostatic potential. In terms of the electron-positron correlation, however, the octahedral site is less favorable, since the electron density is less there than at the tetrahedral site. When the lattice expands, the open spaces at the octahedral and tetrahedral sites increase their sizes and the electron densities there decrease. Due to a subtle balance between the electrostatic and correlation potentials, it seems that the positron distribution shifts in part to the tetrahedral site. As a result, the positron state at each octahedral site obtains more continuity through the tetrahedral site. This is the reason for the change of the bandwidth. For the change in the gap width, the mechanism would be the same. It is thought that the lattice expansion results in a decrease of the energy difference between the octahedral and the tetrahedral states.

We have also calculated positron lifetimes. The resultant values are 325 ps and 491 ps for the LDA and GGA cases, respectively. We did not distinguish between valence and core electrons. As reported for many other materials, the LDA value is shorter than the experimental values around 400 ps.[5,7,9,10,28–31] One reason is that the core electrons are tightly bound to nuclei and do not effectively screen positrons. Since the system is not metallic, even valence electrons show less screening effect than nearly free electrons, for which the LDA enhancement is constructed. Furthermore, rather low electron density at the interstitial sites may

TABLE III. Fraction f_{in} of positron density distribution inside the C_{60} cage for GGA. Values were evaluated at special points Γ, X, W, L, and K. n represents the band index and E_n is the corresponding energy eigenvalue in eV. Higher fraction values are underlined.

	Γ		X		W		L		K	
n	E_n	f_{in}	E_n	f_{in}	E_n	f_{in}	E_n	f_{in}	E_n	f_{in}
1	0.00	0.010	0.44	0.004	0.44	0.004	0.27	0.006	0.42	0.004
2	1.51	0.004	0.70	0.009	0.85	0.008	0.78	0.012	0.77	0.008
3	1.94	0.012	1.13	0.006	0.85	0.008	1.41	0.005	0.98	0.008
4	2.03	0.005	1.67	0.009	1.66	0.019	1.83	0.006	1.71	0.008
5	2.03	0.005	1.67	0.009	2.26	0.006	1.83	0.006	1.93	0.018
6	2.03	0.005	2.90	0.767	2.26	0.006	2.61	0.010	2.65	0.005
7	2.34	0.008	3.16	0.004	3.00	0.949	2.61	0.010	2.94	0.005
8	2.34	0.008	3.16	0.003	3.16	0.004	2.72	0.124	2.98	0.883
9	2.34	0.008	3.33	0.005	3.31	0.019	3.07	0.860	3.35	0.088
10	3.05	0.974	3.41	0.223	3.82	0.007	3.73	0.012	3.73	0.005

play a role. In contrast, the GGA value is larger than the experimental values. Such overestimates for the GGA were found for positron binding atoms or ions.[32] As already pointed out in Ref. 32, the GGA parameter $\alpha=0.22$ was determined to reproduce positron lifetimes in rather dense materials. It might be inappropriate for the sparse C_{60} crystal. For reference, we made calculations with $\alpha=0.12$ and obtained a lifetime value of 407 ps, which is closer to the experimental values mentioned above. The band parameters for this case are listed in Table I also in the columns labeled GGA2. These values are somewhat closer to the LDA values.

In summary, we have calculated positron states and lifetimes in the C_{60} crystal based on the self-consistent electronic structure obtained with an *ab initio* LDA calculation. For the electron-positron correlation, both the LDA and GGA expression were tested. In the ground state, positrons are predominantly distributed at the octahedral interstitial sites for both the LDA and GGA cases, though the positron density amplitude at the tetrahedral site is higher in the GGA result. The difference in the positron distribution is reflected in the positron band structure. Because of the better connection between the octahedral and tetrahedral sites, the GGA result shows a larger dispersion for the lowest positron band. The state in which positrons are distributed inside the C_{60} is predicted to be located at ~ 2.4 eV for the LDA or ~ 3.0 eV for the GGA above the ground state.

All the calculations were performed utilizing computing resources at the Tsukuba Advanced Computing Center (TACC) at the National Institute of Advanced Industrial Science and Technology (AIST), under the Ministry of Economy, Trade, and Industry, Japan (METI).

[1] R.M. Fleming, T. Siegrist, P.M. Marsh, B. Hessen, A.R. Kortan, D.W. Murphy, R.C. Haddon, R. Tycko, G. Dabbagh, A.M. Mujsce, M.L. Kaplan, and S.M. Zahurak, in *Clusters and Cluster-Assembled Materials*, edited by R.S. Averback, J. Bernholc, and D.L. Nelson Mater. Res. Soc. Symp. Proc. 206 (MRS, Pittsburgh, 1991), p. 691.
[2] M.J. Puska and R.M. Nieminen, J. Phys.: Condens. Matter **4**, L149 (1992).
[3] S. Ishibashi, N. Terada, M. Tokumoto, N. Kinoshita, and H. Ihara, J. Phys.: Condens. Matter **4**, L169 (1992).
[4] P.A. Sterne, J.E. Pask, and B.M. Klein, Appl. Surf. Sci. **149**, 238 (1999).
[5] Y. Lou, X. Lu, G.H. Dai, W.Y. Ching, Y.-N. Xu, M.-Z. Huang, P.K. Tseng, Y.C. Jean, R.L. Meng, P.H. Hor, and C.W. Chu, Phys. Rev. B **46**, 2644 (1992).
[6] S. Ishibashi, Mater. Sci. Forum **255-257**, 542 (1997).
[7] Y.C. Jean, X. Lu, Y. Lou, A. Bharathi, C.S. Sundar, Y. Lyu, P.H. Hor, and C.W. Chu, Phys. Rev. B **45**, 12 126 (1992).
[8] J. Krištiak, K. Krištiaková, and O. Šauša, Phys. Rev. B **50**, 2792 (1994).
[9] J.W. Dykes, W.D. Mosley, P.A. Sterne, J.Z. Liu, R.N. Shelton, and R.H. Howell, Chem. Phys. Lett. **323**, 22 (1995).
[10] C.S. Sundar, A. Bharathi, M. Premila, P. Gopalan, and Y. Hariharan, Mater. Sci. Forum **255-257**, 199 (1997).
[11] D.R. Hamann, M. Schluter, and C. Chiang, Phys. Rev. Lett. **43**, 1494 (1979).
[12] D.M. Ceperley and B.J. Alder, Phys. Rev. Lett. **45**, 566 (1980).
[13] J.P. Perdew and A. Zunger, Phys. Rev. B **23**, 5048 (1981).
[14] N. Troullier and J.L. Martins, Phys. Rev. B **43**, 1993 (1991).
[15] L. Kleinman and D.M. Bylander, Phys. Rev. Lett. **48**, 1425 (1982).
[16] S.G. Louie, S. Froyen, and M.L. Cohen, Phys. Rev. B **26**, 1738 (1982).
[17] M.P. Teter, M.C. Payne, and D.C. Allan, Phys. Rev. B **40**, 12 255 (1989).
[18] D.M. Bylander, L. Kleinman, and S. Lee, Phys. Rev. B **42**, 1394 (1990).
[19] G.P. Kerker, Phys. Rev. B **23**, 3082 (1981).
[20] M. Kohyama, Modell. Simul. Mater. Sci. Eng. **4**, 397 (1996).
[21] C.-L. Fu and K.-M. Ho, Phys. Rev. B **28**, 5480 (1983).
[22] S. Ishibashi, N. Terada, M. Tokumoto, N. Kinoshita, and H. Ihara, J. Phys. IV **3(C4)**, 153 (1993).
[23] N. Troullier and J.L. Martins, Phys. Rev. B **46**, 1754 (1992).
[24] E. Boroński and R.M. Nieminen, Phys. Rev. B **34**, 3820 (1986).
[25] B. Barbiellini, M.J. Puska, T. Torsti, and R.M. Nieminen, Phys. Rev. B **51**, 7341 (1995).
[26] B. Barbiellini, M.J. Puska, T. Korhonen, A. Harju, T. Torsti, and R.M. Nieminen, Phys. Rev. B **53**, 16 201 (1996).
[27] S. Ishibashi, J. Phys.: Condens. Matter **14**, 9753 (2002).
[28] T. Azuma, H. Saito, Y. Yamazaki, K. Komaki, Y. Nagashima, H. Watanabe, T. Hyodo, H. Kataura, and N. Kobayashi, J. Phys. Soc. Jpn. **60**, 2812 (1991).
[29] M. Hasegawa, M. Kajino, H. Kuwahara, E. Kuramoto, M. Takenaka, and S. Yamaguchi, Mater. Sci. Forum **105-110**, 1041 (1992).
[30] H.-E. Schaefer, M. Forster, R. Würschum, W. Krätschmer, and D.R. Huffman, Phys. Rev. B **45**, 12 164 (1992).
[31] M. Sano and H. Murakami, Synth. Met. **64**, 315 (1994).
[32] J. Mitroy and B. Barbiellini, Phys. Rev. B **65**, 235103 (2002).